PHYSICAL REVIEW B **83**, 041301(R) (2011)

Spin-orbit fields in asymmetric (001)-oriented GaAs/$Al_xGa_{1-x}As$ quantum wells

P. S. Eldridge,[1,*] J. Hübner,[1] S. Oertel,[1] R. T. Harley,[2] M. Henini,[3] and M. Oestreich[1]

[1]*Institute for Solid State Physics, Leibniz University of Hannover, Appelstrasse 2, D-30167 Hannover, Germany*

[2]*School of Physics and Astronomy, University of Southampton, Southampton, SO17 1BJ, United Kingdom*

[3]*School of Physics and Astronomy, University of Nottingham, Nottingham, NG7 4RD, United Kingdom*

(Received 19 November 2010; published 13 January 2011)

We measure simultaneously the in-plane electron g factor and spin-relaxation rate in a series of undoped inversion-asymmetric (001)-oriented GaAs/AlGaAs quantum wells by spin-quantum beat spectroscopy. In combination the two quantities reveal the absolute values of both the Rashba and the Dresselhaus coefficients and prove that the Rashba coefficient can be negligibly small despite huge conduction-band potential gradients which break the inversion symmetry. The negligible Rashba coefficient is a consequence of the "isomorphism" of conduction- and valence-band potentials in quantum systems where the asymmetry is solely produced by alloy variations.

DOI: 10.1103/PhysRevB.83.041301 PACS number(s): 71.70.Ej

Symmetry is a thread which runs through all of physics, and symmetry reduction discloses basic physical principles. We employ crystallographically engineered symmetry reduction to study the intricate effects of spin-orbit interaction on the electron spin in semiconductor nanostructures. Symmetry reduction is an especially powerful tool in semiconductor physics because the variety of crystallographic directions combined with band-gap engineering allows enormous freedom.

The interplay between structure, symmetry, and electron spin in semiconductors directly affects the spin-relaxation rate Γ_s and the effective electron Landé factor g. Early studies of Γ_s and g focused on bulk zinc-blende material where both entities are isotropic.[1] Subsequently, the reduction in symmetry from T_d to D_{2d} symmetry in symmetrical (001)-oriented quantum wells (QWs) was shown to give rise to anisotropy between the in-plane (x,y) and the out-of-plane (z) directions.[2,3] Further reduction in symmetry to C_{2v} is achieved in (001) quantum wells by removing the mirror symmetry of the quantum well potential and allows an in-plane, twofold symmetric anisotropy of both Γ_s (Ref. 4) and g.[5]

Fundamentally, Γ_s and g are both determined by spin-orbit interaction but the basic mechanisms for their anisotropies are quite different. Theoretically the in-plane anisotropy of g is proportional to the asymmetry of the electron wave function in the z direction with the proportionality constant given by the Dresselhaus or bulk inversion asymmetry (BIA) spin-splitting coefficient γ.[5,6] In contrast, Γ_s is in many cases dominated by the Dyakonov-Perel (DP) spin-relaxation mechanism and the related in-plane anisotropy depends on the ratio (α/β) of the Rashba structural inversion asymmetry (SIA) to the BIA spin splitting.[4] The SIA component is determined in a rather subtle way by the asymmetry of the *structure* along the z direction.[7,8]

In this work, we determine the absolute value of both the Rashba and Dresselhaus coefficients for a series of quantum well structures by simultaneously measuring the in-plane anisotropy of Γ_s and g by spin quantum beat spectroscopy.[9] The specially designed undoped (001) quantum well samples, with reduced C_{2v} symmetry but *without* external electric fields, illustrate clearly the different origins of the two anisotropies as they possess a strong anisotropy of g and nearly negligible anisotropy of Γ_s.

Anisotropies of Γ_s and g have been measured previously in symmetrically grown quantum wells in an external electric field,[10,11] but the decisive simultaneous evaluation of Dresselhaus and Rashba components has not been carried out so far. Hanle measurements in undoped asymmetric quantum wells without an applied electric field have revealed a strong in-plane anisotropy of the Hanle depolarization curve,[12] but such measurements do not distinguish between the anisotropies of Γ_s and g.[13] Recently, Ganichev and co-workers introduced a seminal technique that uses the angular distribution of the spin-galvanic effect and therewith measured the *ratio* of the Rashba and Dresselhaus coefficients in doped quantum wells.[14,15] Salis and co-workers developed a technique that in principle yields the absolute values of the coefficients in doped structures by optically monitoring the angular dependence of the electrons' spin precession.[16] However, screening effects can produce an uncertainty in the measured values.[17]

We first summarize the theoretical mechanisms for g and Γ_s anisotropy.[4,5] For g a small magnetic field in the x direction B_x deflects the rapid zero-point motion of an electron quantized in the z direction and yields a change of momentum in the y direction. This additional momentum δp_y changes the effective Rashba $\mathbf{\Omega_R}$ and Dresselhaus $\mathbf{\Omega_D}$ precession vectors which read for (001) quantum wells in zinc-blende crystals

$$\mathbf{\Omega}_R(\mathbf{p}) = \alpha/\hbar^2 \begin{pmatrix} p_y \\ -p_x \\ 0 \end{pmatrix}, \quad \mathbf{\Omega}_D(\mathbf{p}) = \beta/\hbar^2 \begin{pmatrix} -p_x \\ p_y \\ 0 \end{pmatrix}, \quad (1)$$

where α and β are coefficients and $p_{x,y,z}$ are the components of the electron momentum. Inspection of Eq. (1) shows that $\mathbf{\Omega_R}$ converts δp_y into an additional magnetic field which is parallel to the external magnetic field B_x and thereby alters the diagonal component of the g tensor ($g_{xx} = g_{yy}$). By contrast, $\mathbf{\Omega_D}$ converts δp_y to an additional magnetic field in the y direction, i.e., perpendicular to B_x, and thereby generates an off-diagonal component g_{xy}. A rigorous theoretical treatment yields[5]

$$g_{xy} = g_{yx} = (2\gamma e/\hbar^3\mu_B)\left(\left\langle p_z^2\right\rangle\langle z\rangle - \left\langle p_z^2 z\right\rangle\right), \quad (2)$$

where μ_B is the Bohr magneton and $\langle\,\rangle$ represents an expectation value for the electron wave function. The two

terms in Eq. (2) cancel and g_{xy} vanishes if the electron wave function is symmetric. The anisotropy of the g tensor is thus proportional to the Dresselhaus coefficient γ and determined by asymmetry of the electron wave function, which may be induced by asymmetry of the confining (conduction band) potential for the electrons. The effective g factor for magnetic field oriented at angle ϕ to the (100) axis in the quantum well plane is given by

$$g(\phi) = -\sqrt{g_{xx}^2 + g_{xy}^2 + 2g_{xx}g_{xy}\sin(2\phi)}. \quad (3)$$

For the spin relaxation, which is dominated by the DP mechanism, the rate in the quantum well plane $\Gamma_s^{xy}(\phi)$ is proportional to $\langle \mathbf{\Omega^2} \rangle$ where $\mathbf{\Omega} = \mathbf{\Omega_D} + \mathbf{\Omega_R}$. It will be anisotropic as a result of interference of the components and is given by[4]

$$\Gamma_s^{xy}(\phi) = \frac{C}{2}[\alpha^2 + \beta^2 + 2\alpha\beta\sin(2\phi)], \quad (4)$$

where C is a constant which depends on the in-plane electron momentum relaxation time. Thus the spin-relaxation rate anisotropy gives the ratio α/β, where $\beta = \langle p_z \rangle^2 \gamma/\hbar^2$.

Experimentally, we measure the electron-spin-relaxation rate along the growth direction (z) for a magnetic field applied in the quantum well plane. The magnetic field causes rapid Larmor precession of the electron spins and the measured relaxation rate is given by the average of $\Gamma_s^z = C(\alpha^2 + \beta^2)$ and $\Gamma_s^{xy}(\phi)$ (Ref. 11):

$$\Gamma_s(\phi) = \frac{1}{2}\left[\Gamma_s^z + \Gamma_s^{xy}(\phi)\right] = D\left[1 + \left(\frac{\alpha}{\beta}\right)^2 + \frac{2\alpha}{3\beta}\sin(2\phi)\right], \quad (5)$$

where $D = 3C\beta^2/4$. Therefore measurement of both anisotropies yields simultaneously the absolute values of α and β.

The samples are four molecular beam epitaxy grown, (001)-oriented GaAs/AlGaAs multiple quantum wells with varying asymmetry. Sample A comprises five repeats of a 12-nm $Al_{0.4}Ga_{0.6}As$ barrier, an 8-nm GaAs quantum well followed by a 30-nm alloy layer where the aluminium concentration is varied linearly from 0.04 to 0.4. Samples B–D are equivalent structures but the one-sided potential gradient is in the quantum well and has been grown as a digital alloy with conduction-band gradients equivalent to an electric field of 100 kV/cm (sample B), 50 kV/cm (sample C), and 25 kV/cm (sample D). Figure 1 shows the calculated $n = 1$ electron states for samples A and B obtained by numerical solution of the Schrödinger equation. The calculated confinement energies for electrons in samples A–D are 34, 91, 61, and 37 meV, respectively.

The samples are mounted on a rotation stage in a liquid-helium flow cryostat in a superconducting magnet with the magnetic field oriented in Voigt geometry. The rotation axis corresponds to the growth axis of the sample and is parallel to the direction of excitation. Spin oriented electrons are optically created by circularly polarized ps pulses from a mode-locked Ti:sapphire laser with a repetition rate of 80 MHz, a laser wavelength of 740 nm, and a pulse intensity yielding excitation density $\approx 2 \times 10^{10}$ cm^{-2}. After excitation the carrier momentum distribution rapidly thermalizes by emission of phonons and scattering with other carriers and

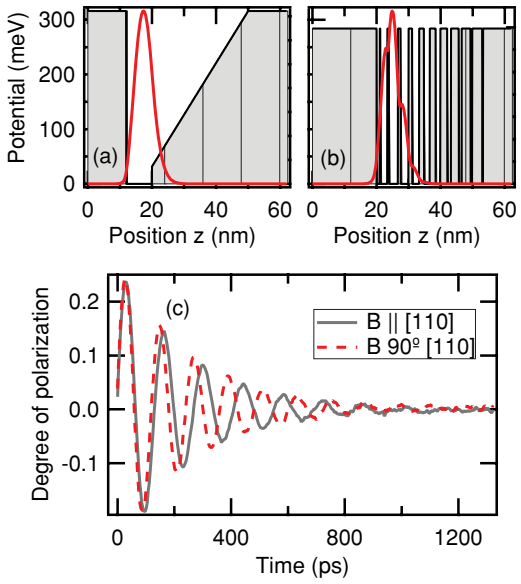

FIG. 1. (Color online) Conduction-band potential profile and numerical calculated electron wave function for the $n = 1$ states for (a) sample A and (b) sample B. (c) The measured spin quantum beats at 125 K for sample A for 3 T in-plane magnetic field clearly showing the different electron g factors for $B\|[110]$ and $[1\bar{1}0]$ and similar spin-relaxation times.

the holes lose their spin orientation within the momentum relaxation time due to strong valence-band mixing and k-dependent spin splitting. The photo-luminescence (PL) is spectrally and temporally resolved by a spectrometer and a synchroscan streak camera with two-dimensional readout with a resolution of 0.5 nm and 8 ps, respectively. The degree of circular polarization of the PL, which is proportional to the electron-spin polarization, is measured by a switchable liquid-crystal retarder and a polarizer.

Figure 1(c) depicts the time evolution of the degree of circular polarization for sample A at 3 T and 125 K for an in-plane magnetic field B along [110] and $[1\bar{1}0]$ directions. The observed oscillations are electron-spin quantum beats, the frequency being $\omega_L = g\mu_B\hbar^{-1}B$, and so are a direct measure of g for the particular magnetic-field direction.[9] Measurements of beats in $\langle S_z \rangle$ in this way do not yield the sign of g but a comparison with previous measurements on symmetric QWs identifies that g is negative for samples A, C, and D and positive for sample B.[10,18] The two clearly distinct oscillation frequencies in Fig. 1(c) directly demonstrate the in-plane g anisotropy whereas the nearly identical decay of the two polarization transients indicate that Γ_s is nearly isotropic.

Figure 2 shows in more detail the dependence of g and Γ_s on the direction of the magnetic field in samples A and B. The black (red online) solid curves in Fig. 2 depict fits of the anisotropy of g using Eq. (3), which directly yield both g_{xx} and g_{xy}. The diagonal components of the g tensor $g_{xx} = g_{yy}$ have been previously investigated in symmetrical quantum wells where the dependence on well width, i.e., confinement energy and barrier penetration, is well described by $k \cdot p$ theory.[18,19] The solid squares in Fig. 3(a) show g_{xx} for all four samples,

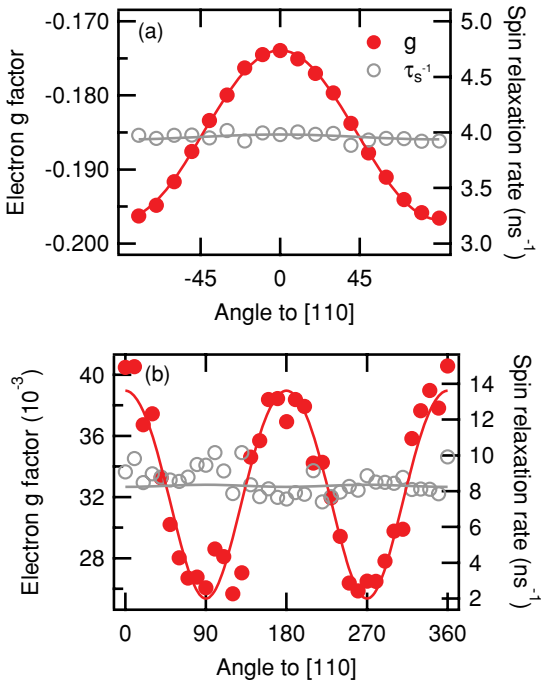

FIG. 2. (Color online) Extracted spin-relaxation rate and electron g factor for different magnetic-field orientations from fits to the spin quantum beat measurements for (a) sample A at 125 K and (b) sample B at 25 K.

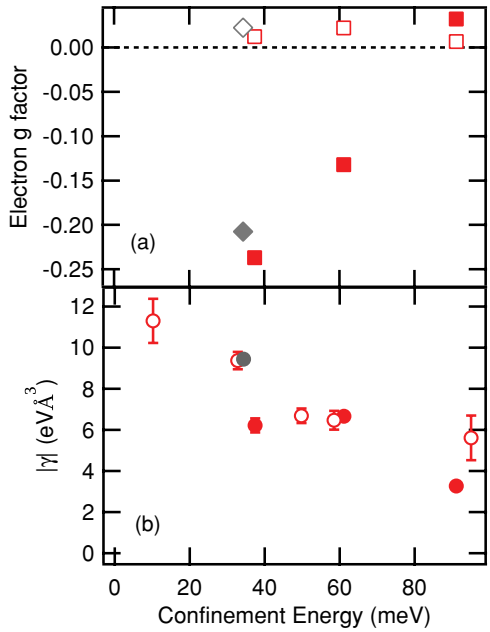

FIG. 3. (Color online) (a)Variation in g_{xx} (solid squares) and g_{xy} (open squares) with confinement energy for samples B and C (5–25 K) and sample A (25 K) (gray diamonds). (b) Experimental values of the Dresselhaus spin splitting constant against confinement energy (solid circles); open circles correspond to data from Ref. 20.

confirming a similar strong dependence of g_{xx} on confinement energy for asymmetric QWs. The open squares in Fig. 3(a) show g_{xy} and these values yield, by Eq. (2), the dependence of the Dresselhaus spin splitting constant γ on confinement energy [solid dots in Fig. 3(b)]. The excellent agreement with data from Ref. 20 illustrates clearly that g_{xy} provides an accurate measure of γ in asymmetric (001) quantum wells. The remaining deviations of γ from the trend probably result from differences between the actual and the nominal sample structures which lead to uncertainties in the calculation of the wave-function asymmetry. Theoretical analysis of the decrease of γ with confinement energy is beyond the scope of this paper. Nonetheless, such a trend is expected from $k \cdot p$ theory and has similar origin to the change of g_{xx} with confinement energy in Fig. 3(a).[7,20]

Next, we study in detail the anisotropy of the spin-relaxation rate. The open circles in Figs. 2(a) and 2(b) depict $\Gamma_s(\phi)$ for samples A and B, respectively, and the gray solid curves are fits according to Eq. (5). Additional temperature- and density-dependent measurements confirm that the DP spin-relaxation mechanism dominates Γ_s. The measurements clearly show that there is almost no in-plane anisotropy of Γ_s and therefore α is close to zero even though the potential gradients in both samples are large (>90 kV/cm).

Figure 4 compares α in our samples (solid circles) with previous experiments in external and internal (Hartree) electric fields (open circles).[21,22] The comparison of the measurements clearly show that the Rashba spin splitting in AlGaAs heterostructures is large even for a modest external (or internal) electric field, but almost negligibly small in the case of asymmetries produced by alloy variation. Although allowed to be nonzero by the C_{2v} symmetry of the samples, the values of α that are required to fit the present data are zero within experimental uncertainties; they show both positive and negative values with no clear trend and the value of α/β is in all cases less than 0.1. The measurements push down by an order of magnitude the previous upper limit of Rashba spin splitting observed in samples with asymmetry from alloy variation.[8,23] The small values of α are a direct consequence of the isomorphous band edges, that is, the conduction- and valence-band potentials are related by a constant factor. This is due to the fact that the expectation value of the effective electric field always vanishes in the conduction band due to Ehrenfest's theorem,[7] *and* in isomorphous structures, as illustrated in the right-hand panel of Fig. 4, it will also vanish in the valence band, and it is the latter which determines the spin splitting.

In conclusion, we have determined simultaneously the absolute values for the Dresselhaus and the Rashba spin-orbit interaction in undoped low-symmetry (001) quantum wells. All samples show a distinctive anisotropy of the electron g factor but essentially isotropic spin-relaxation rates. This difference highlights the different origins of the two phenomena; the first is a measure of the conduction electron wave-function asymmetry and the latter is a measure of the expectation value of the valence-band potential on conduction-band states. Although a one-sided gradient of the conduction and/or valence band leads in general to a finite Rashba spin-orbit interaction, the experiment proves that isomorphism of the valence and conduction band in GaAs/AlGaAs quantum wells proscribe a sizable, gradient-induced Rashba spin-orbit splitting.

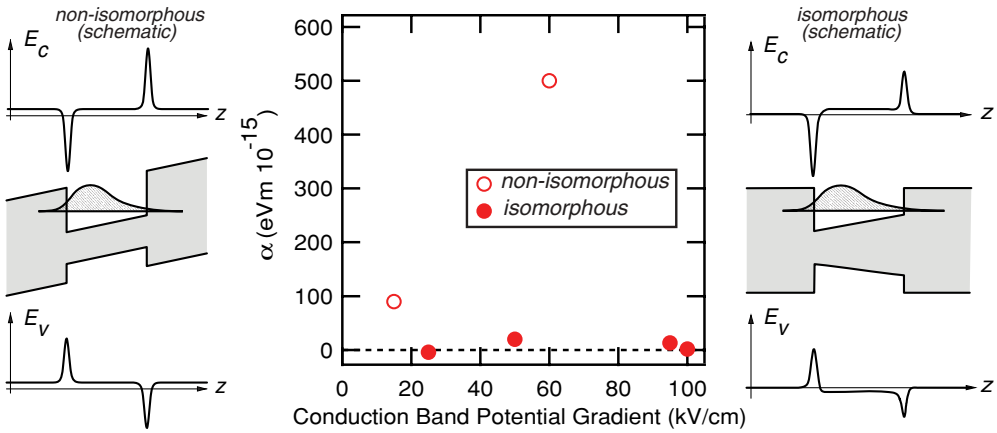

FIG. 4. (Color online) Extracted values of the Rashba spin-orbit constant vs conduction-band potential gradient for samples A–D (solid circles). The open circles show values for a built-in Hartree electric field (Ref. 21) of ∼15 kV/cm in an *n*-modulation doped structure and for an externally applied electric field of 60 kV/cm in an undoped (110)-oriented multiple quantum well sample (Ref. 22). Right and left panels show schematic potential profiles and electron probability density (middle) and effective electric field for conduction (top) and valence bands (bottom) (after Ref. 7). For an "isomorphous" structure (right panel) the expectation value of the valence-band electric field will vanish but *not* for a "nonisomorphous" structure (left panel), giving zero (finite) SIA spin splitting for the former (latter) (Ref. 8).

We thank K. Köhler for providing us with the samples and W. W. Rühle for helpful discussions. We gratefully acknowledge financial support from Engineering and Physical Sciences Research Council (EPSRC) and from the Deutsche Forschungsgemeinschaft in the framework of the priority programm "SPP 1285 - Semiconductor Spintronics" and the excellence cluster "QUEST - Center for Quantum Engineering and Space-Time Research."

*Author to whom correspondence should be addressed. eldridge@nano.uni-hannover.de

[1] *Optical Orientation*, Modern Problems in Condensed Matter Science Vol. 8, edited by F. Meier and B. Zakharchenya (North-Holland, Amsterdam, 1984).

[2] E. L. Ivchenko and A. A. Kiselev, Sov. Phys. Semicond. **26**, 827 (1992).

[3] M. I. Dyakonov and V. Y. Kachorovskii, Sov. Phys. Semicond. **20**, 110 (1986).

[4] N. S. Averkiev and L. E. Golub, Phys. Rev. B **60**, 15582 (1999).

[5] V. K. Kalevich and V. L. Korenev, JETP Lett. **57**, 571 (1993).

[6] G. Dresselhaus, Phys. Rev. **100**, 580 (1955).

[7] R. Winkler, *Spin-orbit Coupling Effects in Two-Dimensional Electron and Hole Systems* (Springer, Berlin, 2003).

[8] P. S. Eldridge, W. J. H. Leyland, P. G. Lagoudakis, R. T. Harley, R. T. Phillips, R. Winkler, M. Henini, and D. Taylor, Phys. Rev. B **82**, 045317 (2010).

[9] A. P. Heberle, W. W. Rühle, and K. Ploog, Phys. Rev. Lett. **72**, 3887 (1994).

[10] M. Oestreich, S. Hallstein, and W. Rühle, IEEE J. Sel. Top. Quantum Electron. **2**, 747 (1996).

[11] A. V. Larionov and L. E. Golub, Phys. Rev. B **78**, 033302 (2008).

[12] N. S. Averkiev, L. E. Golub, A. S. Gurevich, V. P. Evtikhiev, V. P. Kochereshko, A. V. Platonov, A. S. Shkolnik, and Y. P. Efimov, Phys. Rev. B **74**, 033305 (2006).

[13] W. Hanle, Z. Phys. A: Hadrons Nucl. **30**, 93 (1924).

[14] S. D. Ganichev, E. L. Ivchenko, V. V. Bel'kov, S. A. Tarasenko, M. Sollinger, D. Weiss, W. Wegscheider, and W. Prettl, Nature (London) **417**, 153 (2002).

[15] S. D. Ganichev *et al.*, Phys. Rev. Lett. **92**, 256601 (2004).

[16] L. Meier, G. Salis, I. Shorubalko, E. Gini, S. Schön, and K. Ensslin, Nature Phys. **3**, 650 (2007).

[17] M. Studer, S. Schön, K. Ensslin, and G. Salis, Phys. Rev. B **79**, 045302 (2009).

[18] M. J. Snelling, G. P. Flinn, A. S. Plaut, R. T. Harley, A. C. Tropper, R. Eccleston, and C. C. Phillips, Phys. Rev. B **44**, 11345 (1991).

[19] R. M. Hannak, M. Oestreich, A. P. Heberle, W. W. Rühle, and K. Köhler, Solid State Commun. **93**, 313 (1995).

[20] W. J. H. Leyland, R. T. Harley, M. Henini, A. J. Shields, I. Farrer, and D. A. Ritchie, Phys. Rev. B **76**, 195305 (2007).

[21] D. Stich, J. H. Jiang, T. Korn, R. Schulz, D. Schuh, W. Wegscheider, M. W. Wu, and C. Schüller, Phys. Rev. B **76**, 073309 (2007).

[22] P. S. Eldridge, W. J. H. Leyland, P. G. Lagoudakis, O. Z. Karimov, M. Henini, D. Taylor, R. T. Phillips, and R. T. Harley, Phys. Rev. B **77**, 125344 (2008).

[23] They also provide an experimental upper limit to the magnitude of spin-orbit splitting induced by the effective mass gradient highlighted in recent theoretical work by A. Matos-Abigue, Phys. Rev. B **81**, 165309 (2010).